# Synthesis of CuO Nanoparticles for Adsorbent of Methylene Blue

Dani Gustaman Syarif [1], Hasniah Aliah [2], Jakaria Usman [13], Yofi Ike Pratiwi [4]
{danigus@batan.go.id[1], }

Center for Applied Nuclear Science and Technology-BATAN,
Jl. Tamansari 71, Bandung 40132, Indonesia[1, 3, 4]
Physics Department, Saintech Faculty, UIN Sunan Gunung Djati, Bandung[2]

**Abstract.** Nanoparticles of CuO have been synthesized using precipitation method for methylene blue adsorbents. Copper chloride was used as precursor. Powder of copper chloride was dissolved in water and then precipitated using NaOH. The precipitate was dried and after that it was calcined at 300-500ºC for 2 hours. The CuO nanoparticles was analyzed using X-ray diffraction (XRD). The specific surface area of the nanoparticles was measured using a surface area meter. The adsorbance of the CuO nanoparticles was tested by utilizing methylene blue as an example of dye waste. According to XRD data, all CuO nanoparticles calcined at 300-500ºC were monoclinic with crystallite size 17-32.8 nm. The specific surface areas of the CuO nanoparticles were 26, 36, and 77.6 $m^2/g$ for calcination temperature of 500, 400, and 300ºC that correspond to the particle size of 36.5, 26.4, and 12.2 nm. The best adsorbent for methylene blue was the CuO nanoparticles calcined at 400ºC for 2 hours with an adsorption capacity of 61 mg/g at pH 7.

**Keywords:** Adsorbent, CuO nanoparticles, methylene blue (MB), wastewater, pollution.

## 1. Introduction

Along with the times, human needs continue to grow. Various products continue to be produced to meet those needs. Some of the products that continue to grow are textile, leather, and paper products. In its production, textiles, leather, and paper use coloring agents (dyes) [1] [2] [3]. A side effect of dyes in producing textiles, leather and paper is the production of liquid waste containing dyes (wastewater) [1] [2] [3] [4]. Wastewater causes environmental pollution problems when released into the water and soil environment. The dyes that are consumed can cause various diseases and those released into the soil and water can also block the penetration of sunlight needed for important processes including photosynthesis [1] [4].

Various efforts to overcome the problem of contamination due to dyes have been and are being carried out using various methods including using adsorbents and photocatalysts [5]. The use of adsorbent is mostly done because the manufacturing is relatively easy and inexpensive, and the raw materials are available abundantly such as biomass and ceramics[1] [2] [3] [4] [5] [6]. The use of ceramics for adsorbents is very beneficial because it can be used repeatedly while the use of carbon from biomass cannot be used repeatedly. Various ceramics can be made into adsorbents such as

ICONISTECH 2019, July 11-12, Bandung, Indonesia

DOI 10.4108/eai.11-7-2019.2297422

$Al_2O_3$ [5], $Fe_3O_4$][7][8], and CuO [9] [10] [11]. The use of CuO as adsorbent of methylene blue (MB) is relatively rare, one of which was carried out by Mustafa et al. [10], however, the informations were not described clearly, especially the data related to the adsorption capacity. CuO is very interesting to be used as an adsorbent because it can be made from Cu containing-waste originally from electronics, power lines, telecommunication cables, railways cables, electric appliances, machines, automobiles, industrial machines and buildings.

In this study, CuO nanoparticles were synthesized for adsorbent of MB as one of the waste dyes using a simple method namely precipitation. The synthesis was carried out at a relatively low temperature to determine the lowest calcination temperature that can produce CuO nanopaticles with a relatively large adsorption capacity. In addition, the motivation of this research is to be able to produce CuO adsorbents for dye from Cu containing-wastes, in the future.

## 2. Methodology

### 2.1 Synthesis and Characterization of CuO nanoparticles

Powder of $CuCl_2$-$2H_2O$ was diluted in water placed in a beaker glass. The solution was then precipitated by adding $NH_4OH$ solution into it slowly. The precipitate was washed using water and then calcined at 300$^o$C, 400$^o$C, and 500$^o$C for 2 hours. Calcined products were crushed to obtain CuO nanoparticles powder. Analysis using XRD was then carried out to determine the crystal structure and phases that were formed. The specific surface area and adsorption-desorption characteristics of CuO nanoparticles were measured using a Quantachrome's surface areameter. Surface characteristics of nanoparticles were also studied using an FTIR. The morphology of the CuO nanoparticles was examined using a SEM.

### 2.2 Adsorbence testing

The adsorbance test was carried out using commercial methylene blue as an example of dye waste. To find out the samples that have the largest adsorption capacity, three samples of CuO calcined at temperatures of 300$^o$C, 400$^o$C, and 500$^o$C were tested using an MB solution with a concentration of 20 ppm at pH 7. A total of 5 mg CuO powder was put into the MB solution and then stirred with magnetic stir for 10 minutes. After stirring, a portion of the MB solution was taken out and centrifuged for 15 minutes. Its adsorbance was measured using a UV-Vis spectrometer at a wavelength of 657 nm. This experiment was conducted for all three types of CuO samples. The best sample obtained was tested using an MB solution of 20 ppm at pH 4, 7, and 9 to determine their adsorption capacity at different pHs. Next, in order to determine the adsorption kinetics of the best sample, the experiment was carried out as follows. The amount of 5 mg of CuO powder from the best type of sample was put into the MB solution with a concentration of 10 ppm and 20 ppm

then stirred with a magnetic stirrer. At each time interval of 10, 20, 30, 60, and 120 minutes a portion of the solution was taken out and centrifuged for 15 minutes. After centrifuging, the adsorption was measured using a UV-Vis spectrometer. After that, to find out the adsorption characteristics of CuO samples and at the same time to find out the largest adsorption capacity, an experiment was carried out as follows. A total of 5 mg of CuO sample was put into 20 ml of MB solution with concentrations of 10, 20, 30, 40, and 50 mg / L and then stirred with a magnetic stirrer for 10 minutes. After that, some of it was taken out and centrifuged for 15 minutes. After centrifugation, the adsorbance was measured using the UV-Vis spectrometer.

## 3 Results and discussion

### 3.1 XRD analyses

Diffraction patterns of CuO nanoparticles calcined at temperatures of 300°C, 400°C, and 500°C are shown in Fig. 1-3. All diffraction patterns exhibit the same diffraction pattern consisting of broad diffraction peaks. In all three diffraction patterns it is clear that there are diffraction peaks at 2θ = 32.5, 35.4, 38.7, 46.5, 48.8, 53.4, 58.3, 61.5, 65.8, 66.2, 68, 72.5 and 75.2. After comparing with the JCPDS standard diffraction pattern, it is known that the peaks are related to the crystal plane of (110), (005), (111), (-112), (-202), (020), (202), (-113), (002), (-311), (311), and (004) of the JCPDS standard of CuO diffraction pattern JCPDS 45-0937. The diffraction pattern of CuO nanoparticles synthesized in this work is in accordance with the CuO standard diffraction pattern of JCPDS No. 45-0937. The CuO nanoparticles crystallize in monoclinic structure with C2/c space group. The crystallite size was then measured using the Debye Scherrer equation shown in equation (1) [12]. The calculation results are shown in Table 1. Compared to CuO nanoparticles made by Mustafa at 300°C (Crytallite size 20-28nm)[10], crystallite size of the CuO nanoparticles calcined at the same temperature in this work is smaller (17 nm).

$$CS = \frac{0.9\lambda}{\beta.Cos\theta} \quad \text{.....( 1 )}$$

where $CS$ = Crystallite size (nm), $\lambda$ = the panjang gelombang (nm), $\beta$ =FWHM (radian), dan $\theta$ = the diffraction angle (radian). From Fig. 1-3 it can be seen that the diffraction intensity is higher with the increase in the calcination temperature. This data shows that CuO formation is getting better with increasing calcination temperatures. As shown in Fig. 1 and 2, there is a peak at 2θ =16° that not belonging to CuO, that means that not all precursor converted to CuO during calcination at 300°C. Almost all of the precursor was converted to CuO during calcination at 400°C, shown by

low peak at 2θ =16°. All of the precursor was completely converted to CuO during calcination at 500°C. The crystallite size data in Table 1 shows that the CuO crystallite size enlarges by increasing the calcination temperature. At higher temperatures there is more heat energy to grow crystals.

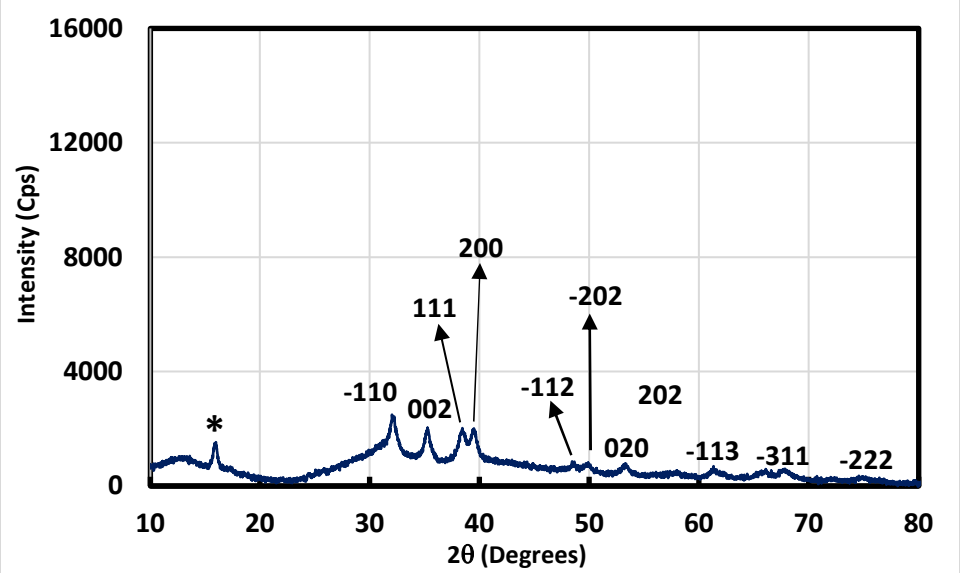


**Fig.1.** XRD pattern of CuO 300°C-2J. CS 17 nm

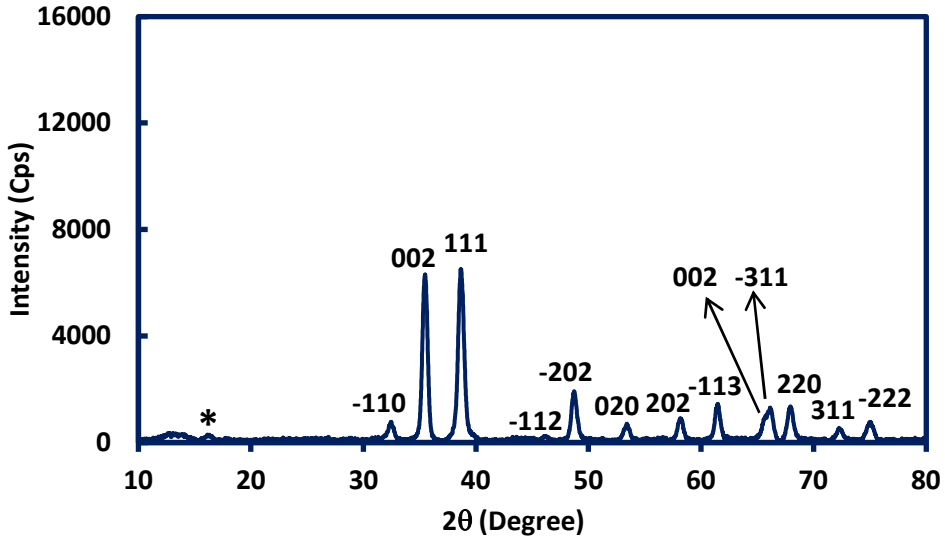


**Fig.2.** XRD pattern of CuO 400ºC-2J. CS 24.4 nm.

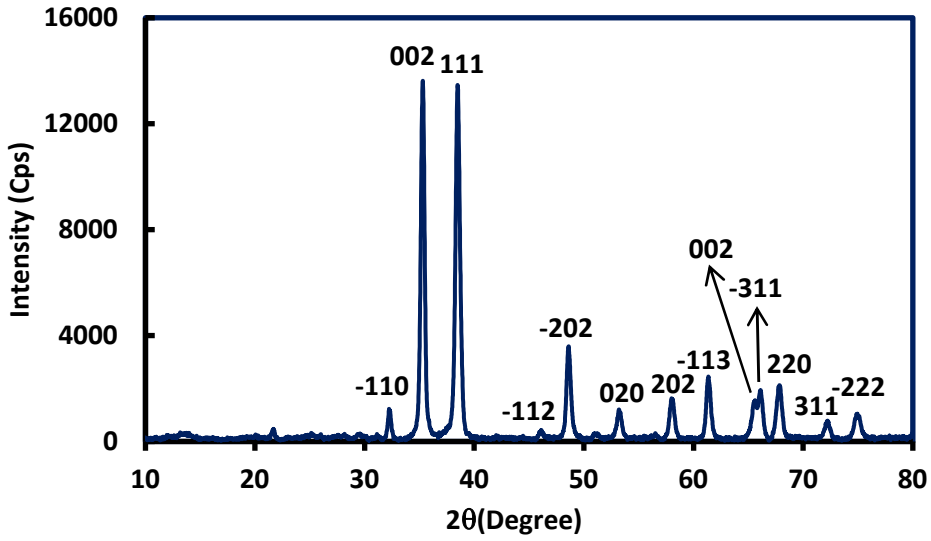


**Fig.3.** XRD pattern of CuO 500ºC-2J. CS 32.8 nm.

## 3.2 Surface area and Adsorption-Desorption analyses

The specific surface area of CuO nanoparticles is shown in Table 1. From this specific surface area data, particle size was obtained using equation 2 and density data of CuO of 6.315 g/cm$^3$. The particle size that was calculated is also displayed in Table 1.

$$D = \frac{6000}{\rho . A} \quad \text{.....( 2 )}$$

dengan $D$ = Particles size (nm), $\rho$ = The density of nanoparticles (g/cm$^3$), and $A$ = The specific surface area of nanoparticles (m$^2$/g).

**Table 1.** Specific surface area, particles size, and crystallite size of CuO nanoparticles.

| No. | Calcination temperature (°C) | Specific surface area (BET) (m$^2$/g) | Particles size (BET) (nm) | Crystallite size (XRD) (nm) |
|---|---|---|---|---|
| 1 | 300 | 77.6 | 12.2 | 17.0 |
| 2 | 400 | 35.6 | 26.4 | 24.4 |
| 3 | 500 | 26.0 | 36.5 | 32.8 |

## 3.3 FTIR Analyses

As can be seen in Fig. 4, there are peaks at 3200-3550 cm$^{-1}$ that is attributed to O-H stretching vibration of surface hydroxyl groups of adsorbed water molecules [13]. This is due to a high surface to volume ratio of the nanoparticles that adsorbs high moisture. The peak at around 1630 cm$^{-1}$ is corresponding to O-H bending vibration due to water absorbed [13]. The height of the peaks corresponding to O-H at position 1630 cm$^{-1}$ and 3200-3550 cm$^{-1}$ decreases with increasing calcination temperature. This indicates that the water attached to the surface of the nanoparticles decreases with increasing calcination temperature. The peaks at below 700 cm$^{-1}$ is due to Cu-O stretching vibration and the peak at 1050-1100 cm$^{-1}$ is attributed to C-OH (C-O stretching 10331/cm [13] stretching. The peak located at wave numbers around 1050-1100 cm$^{-1}$ also decreases with increasing calcination temperature.

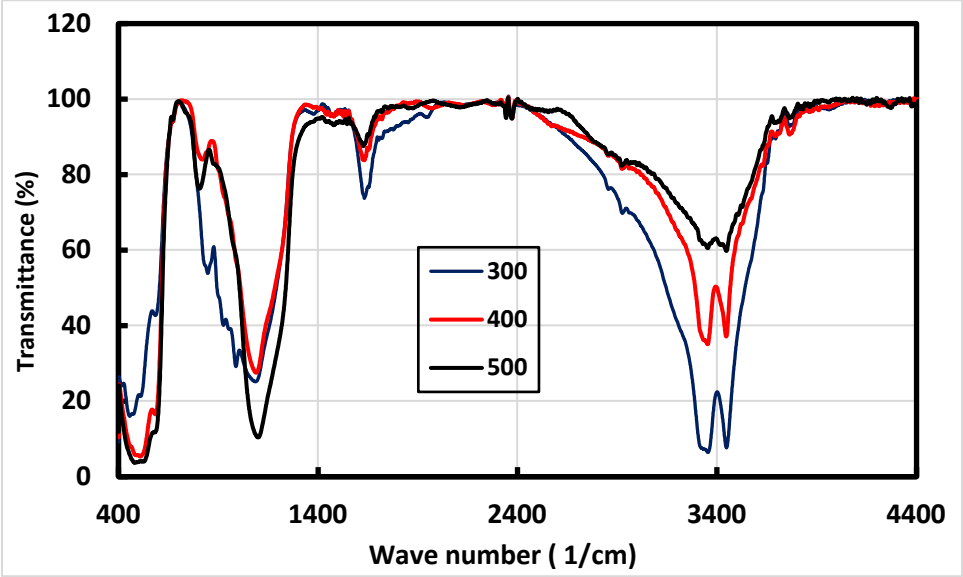


**Fig. 4.** FTIR data for CuO nanoparticles with three different calcination temperatures.

## 3.4 SEM analyses

SEM images of CuO nanoparticles calcined at 300, 400, and 500°C are shown in Fig. 5. As can be seen, the powder has a porous structure. From the scale, it can be predicted that the particle size of the powder is on a nanometer scale, however, it is very difficult to precisely measure the particle size of the image.

## 3.5 Adsorption-Desorption Isotherm

The adsorption-desorption process that has occurred in the CuO adsorbent in this study is shown in Fig. 6. Based on the IUPAC classification, the characteristic of this curve is Type IV, which is a curve that has a hysteresis section. The hysteresis curve formed at low value of P/Po indicates that the CuO adsorbents made contain mesoporous pores with a size of 2-50 nm. If the three adsorption-desorption characteristic curves of the CuO samples calcined at temperatures of 300, 400, and 500°C are compared, it is clear that the largest adsorption volume is possessed by CuO with a calcination temperature of 300°C. The volume of adsorption decreases with increasing calcination temperature according to

data in Table 2. With the calcination temperature rising, the particles get larger and the more interconnections between particles occur, decreasing total pore volume.

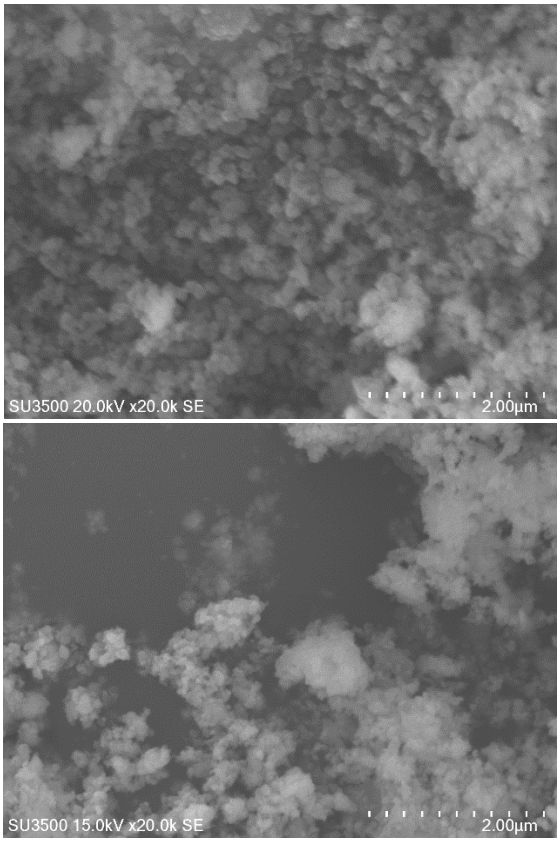


A B

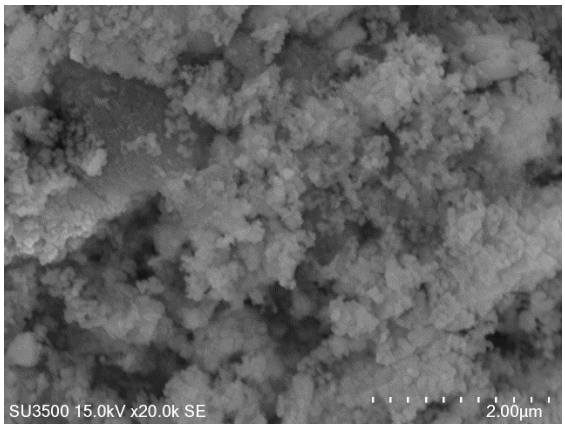


C

**Fig. 5.** SEM images of the CuO nanoparticles calcined at 300ºC (A), 400ºC (B), and 500ºC (C).

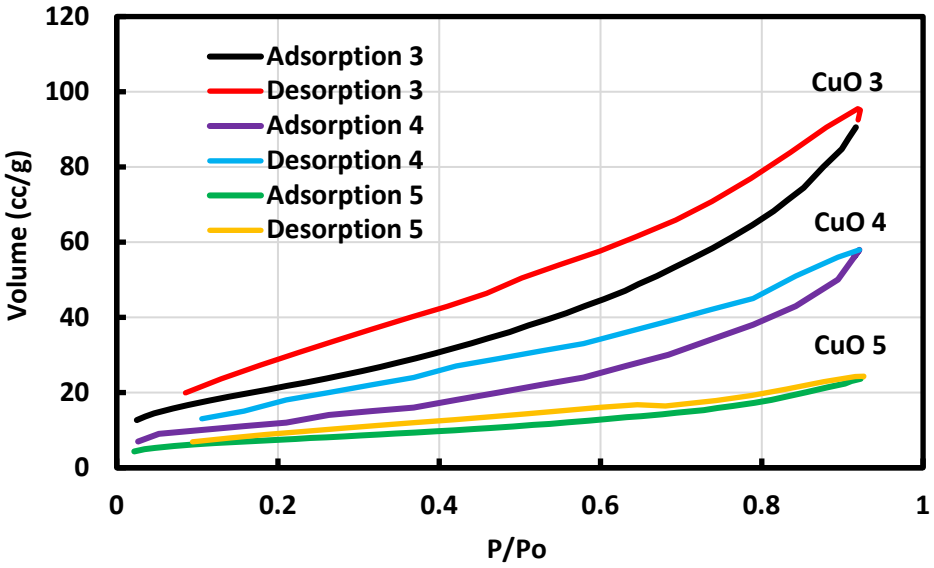


**Fig. 6.** Adsorption-desorption characteristics of the CuO nanoparticles with different calcination temperatures: 300ºC (CuO 3), 400ºC (CuO 4), and 500ºC (CuO 5).

**Table 2.** Total pore volume of CuO nanoparticles.

| No. | Calcination temperature (°C) | Total pore volume (cc/g) |
|---|---|---|
| 1 | 300 | 0.147 |
| 2 | 400 | 0.090 |
| 3 | 500 | 0.038 |

## 3.6 Characteristics of CuO adsorbent

The adsorption capacity of CuO calcined at 300, 400 and 500°C in 20 ml MB solution with concentration of 20 mg/L and pH 7 shown in Table 3. As can be seen in Table 3, the largest adsorption capacity possessed by CuO nanoparticles calcined at 400°C. Based on this data, we examined the CuO calcined at 400°C in MB solution with different pHs namely 4, 7 and 9. The adsorption capacity of the CuO nanoparticles was determined by applying them in 10 ml MB solution having pH 4, 7, and 9. The results of the examination were displayed in Table 3 and 4.

**Table 3.** Adsorption capacity of CuO nanoparticles with different calcination temperature.

| No. | Calcination temperature (°C) | Adsorption capacity (qt) (mg/g) | Note |
|---|---|---|---|
| 1 | 300 | 25.7 | Tested using 20 ml MB solution with concentration of 20 mg/L with contact time of 10 minutes. Concentration of adsorbent is 5 mg. pH=7. |
| 2 | 400 | 47.0 | |
| 3 | 500 | 30.3 | |

**Table 4.** Adsorption capacity of CuO nanoparticles calcined at 400°C with different pHs of the MB solution.

| No. | pH | Adsorption capacity (qt) (mg/g) | Note |
|---|---|---|---|
| 1 | 4 | 18.5 | Tested using 10 ml MB solution with concentration of 20 mg/L with contact time of 10 minutes. Concentration of adsorbent is 5 mg. |
| 2 | 7 | 24.3 | |
| 3 | 9 | 23.9 | |

The adsorption capacity of CuO calcined at 300, 400 and 500°C for 2 hours is shown in Table 3. As seen in Table 3, the adsorption capacity of calcined CuO at 400°C is the largest adsorption capacity, and this is greater than the other adsorption capacity of CuO which is calcined at higher temperatures of 500°C and at lower temperature of 300°C. The adsorption capacity is greater than

that calcined at 500ºC due to the greater surface area and pore volume of CuO. Actually the surface area and pore volume of CuO calcined at 400ºC is smaller than those of the CuO calcined at 300ºC, however, the adsorption capacity of the CuO calcined at 400ºC is greater than that of the CuO calcined at 300ºC. It is due to better CuO formation of the sample calcined at 400ºC. As shown in Fig. 1 and 2, there is a peak at 2θ =16º that not belonging to CuO, that means that a part of the precursor did not convert to CuO during calcination at 300ºC. Whilst almost all of the precursor converted to CuO during calcination at 400ºC. This is shown by lower peak at 2θ =16º. Then, all of the precursor completely converted to CuO during calcination at 500ºC. However, the adsorption capacity of the sample calcined at 500ºC is smaller than that of the sample calcined at 400ºC. The cause is the larger particle size and smaller surface area and pore volume of the sample calcined at 500ºC.

The adsorption capacity of CuO calcined at 400ºC for 2 hours at different pH can be seen in Table 4. The adsorption capacity is smaller when the adsorbent of CuO is applied in acidic MB solution and show good performance as adsorbent when applied in neutral to basic MB solution.

As shown in Fig. 6 and 7, the adsorption capacity increases with the increase in contact time. However, the change stops after reaching the equilibrium time. The kinetic characteristics of adsorption capacity were studied by applying the "Pseudo-first order" and "Pseudo-second order" models represented by equations (3) and (4) [14] [15]. Kinetic characteristics of removal of MB on to CuO nanoparticles parameters of isotherm of the MB adsorption on to CuO nanoparticles are shown in Table 5. As shown in Figures 6 and 7, and Table 5, the data in this study are quite in accordance with "Pseudo-second order". The $R^2$ value of Pseudo second order curve is larger than that of Pseudo first order, and the $R^2$ value of the Pseudo second order curve almost reach 1. This data shows that the MB degradation rate and kinetic adsorption behavior follow a pseudo second order model that describes the ionic exchange process and chemisorption between MB molecules and positive partial charge of the CuO nanoparticles. The kinetic data of Mustafa et al. [10] also follows the pseudo second order model.

$$q_t = q_e(1 - Exp(k_1 t) \quad \text{.....(3)}$$

where, $q_t$ = Adsorption capacity at time t, $q_e$ = Maximum adsorption capacity, t = contact time, and $k_1$ = Constant.

$$\frac{t}{q_t} = \frac{1}{k_2 . q_2^2} + \frac{t}{q_e} \quad \text{.....( 4 )}$$

where, $q_t$ = Adsorption capacity at time t, $q_e$ = Maximum adsorption capacity, t = contact time, and $k_2$ = Constant.

Data on adsorption capacity as a function of the concentration of MB equilibrium are shown in Figure 8. The greater the equilibrium concentration, the greater the adsorption capacity. However, at a certain equilibrium concentration, the adsorption capacity tends to remain and reach equilibrium. Characteristics of changes in adsorption capacity to equilibrium concentrations were studied by applying the Langmuir and Freundlich equations shown in equations (5) and (6) [14] [15].
As can be seen in Fig. 8, the characteristics of the adsorption capacity curve as a function of equilibrium concentration tends to follow the Langmuir equation. Although, the Freundlich equation is nearly fit the data. Based on the $R^2$ value, the $R^2$ value for Langmuir model is 0.94 and that for Freundlich is 0.89. The difference is small. This means that the adsorption of MB molecules on the surface of CuO nanoparticles form a monolayer, however, tends to form multilayer. Based on Langmuir equation, the maximum adsorption capacity of CuO nanoparticles calcined at 400°C is 61 mg/g at pH 7. Compared to other adsorbents depicted in Table 7, the adsorption capacity of the CuO adsorbent made in this work is good enough and comparable.

$$\frac{C_e}{q_e} = \frac{C_e}{q_m} + \frac{1}{q_m . K_L} \quad \text{.....(5)}$$

where $q_e$ = Adsorption capacity at the equilibrium condition (mg/g), $C_e$ = Concentration of adsorbate at equilibrium condition (mg/L), $q_m$ = Maximum adsorption capacity (mg/g), and $K_L$ = The Langmuir adsorption constant (L/mg).

$$\log\ q_e = \log\ K_F + \frac{1}{n} . \log\ C_e \quad \text{.....(6)}$$

where, $K_F$ = The Freundlich adsorption constant (mg/g(L/mg)1/n), $q_e$ = Adsorption capacity at the equilibrium condition (mg/g), $C_e$ = Concentration of adsorbate at equilibrium condition (mg/L), and n is the heterogeneity factor.

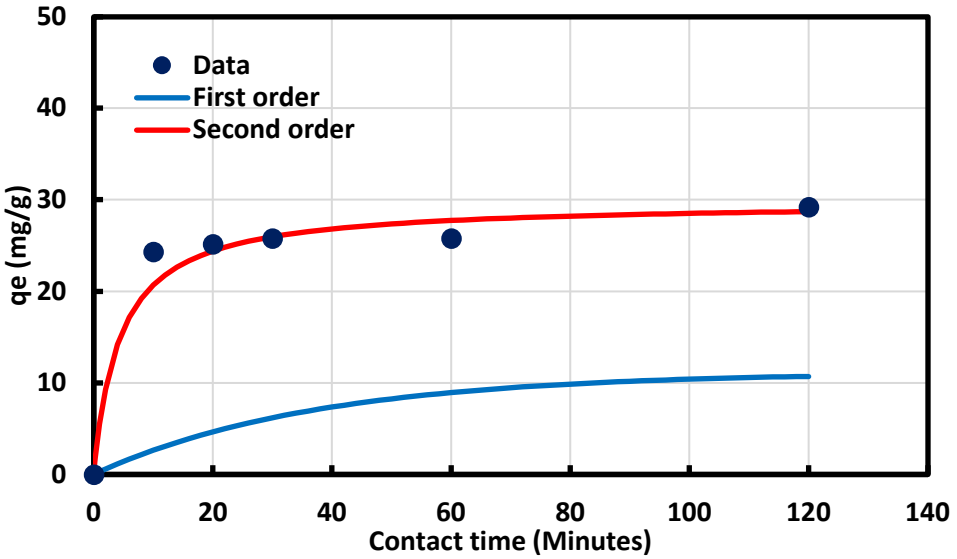


**Fig.7.** Adsorption capacity CuO nanoparticles (Code 4-2) as function of contact time in 10 mg/L Methylene blue solution (pH 7, 5 mg adsorbent).

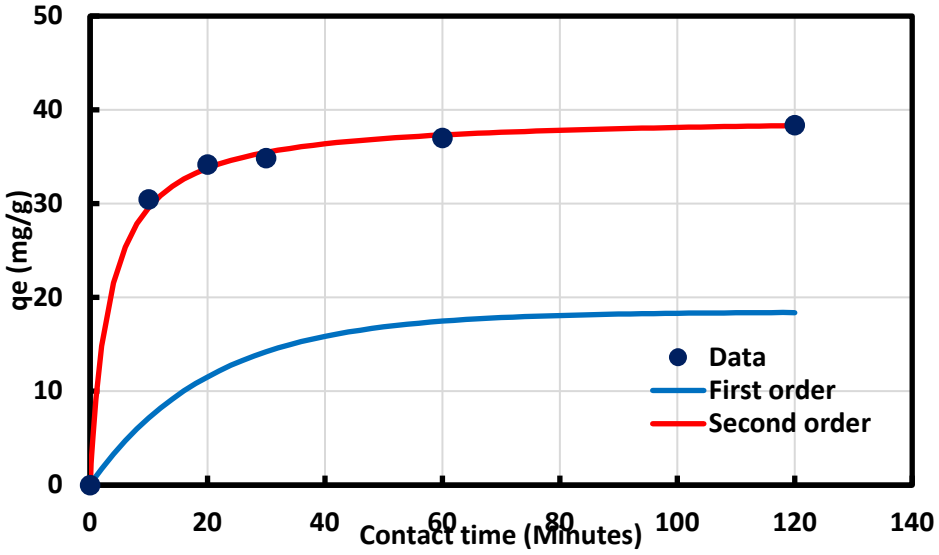


**Fig.8.** Adsorption capacity CuO nanoparticles (Code 4-2) as function of contact time in 20 mg/L Methylene blue solution (pH 7, 5 mg adsorbent).

**Table 5.** Kinetic characteristics of removal of MB on to CuO nanoparticles.

| Isotherm | Parameters | 20ml MB solution with pH 7 | |
|---|---|---|---|
| | | 10 ppm | 20 ppm |
| Second order | $q_e$ (mg/g) | 29.76 | 39.37 |
| | 1/(k2.qe^2) | 0.1479 | 0.0843 |
| | k2 (g/mg min) | 0.007633 | 0.007653 |
| | $R^2$ | 0.9984 | 0.9984 |
| First order | qe (mg/g) | 11.16 | 18.42 |
| | $K_1$ (1/min) | -0.0269 | -0.049 |
| | $R^2$ | 0.8813 | 0.8813 |

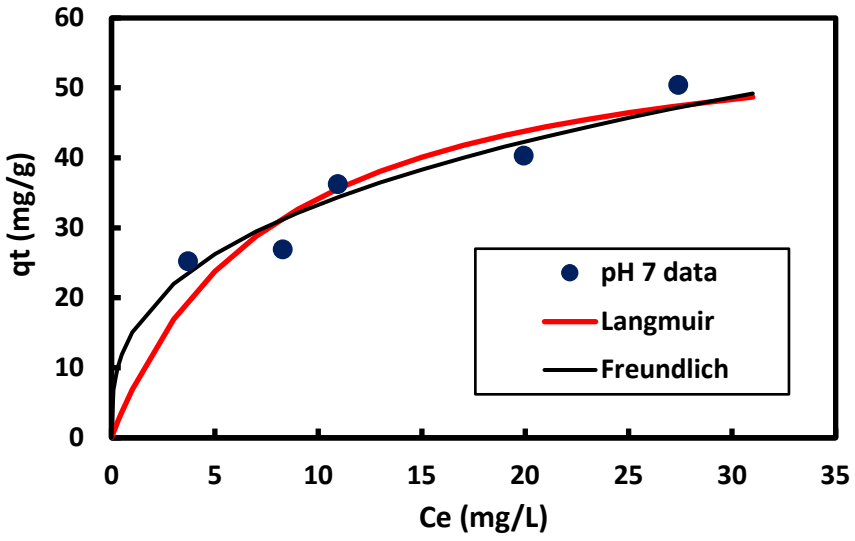


**Fig. 9.** Adsorption capacity (qt) as function of equilibrium concentration (Ce).

**Table 6.** Isotherm parameters for removal of MB (pH 7) on to CuO nanoparticles.

| Isotherm | Parameters | CuO nanoparticles |
|---|---|---|
| | | 400°C |
| Langmuir | $q_m$ (mg/g) | 61 |
| | $K_L$ (L/mg) | 7.82 |
| | $R^2$ | 0.94 |
| Freundlich | $K_F$(mg/g(L/mg)$^{1/n}$) | 15.07 |
| | 1/n | 0.3447 |
| | $R^2$ | 0.89 |

**Table 7.** Maximum MB adsorption capacity of some adsorbents.

| Adsorbent | $q_m$ (mg/g) | Literature |
|---|---|---|
| Cello lignin wastes | 95.2 | [16] |
| Spent tea leaves | 62.2 | [16] |
| Oak sawdust | 29.94 | [16] |
| Rice husk | 40.6 | [16] |
| Almond peel | 77-118 | [16] |
| Wood apple cell | 95.2 | [16] |
| Broad bean peel | 192,7 | [16] |
| Gypsum | 36 | [17] |
| CuO | 61 | This work |

## 4 Conclusion

Powder of CuO nanoparticles for methylene blue adsorbent has been successfully synthesized by precipitation method. The CuO nanoparticles have a monoclinic crystal structure with crystallite sizes of 12.2-36.5 nm. As an adsorbent for methylene blue, CuO nanoparticles in this study have maximum adsorption capacity of 61 mg/g. The optimum calcination temperature for CuO synthesis in this work is 400ºC. Isotherm kinetics of the MB adsorption on the CuO nanoparticles follow the Pseudo second order equation, whilst the adsorption characteristics follow Langmuir equation.

## References


[1] W. Wei, L. Yang, W. H. Zhong, S. Y. Li, J. Cui, and Z. G. Wei, "Fast removal of methylene blue from aqueous solution by adsorption onto poorly crystalline hydroxyapatite nanoparticles," *Dig. J. Nanomater. Biostructures*, 2015.

[2] Z. Salahshoor and A. Shahbazi, "Review of the use of mesoporous silicas for removing dye from textile wastewater," *Eur. J. Environ. Sci.*, 2014, doi: 10.14712/23361964.2014.7.

[3] R. R. Krishni, K. Y. Foo, and B. H. Hameed, "Adsorptive removal of methylene blue using the natural adsorbent-banana leaves," *Desalin. Water Treat.*, 2014, doi: 10.1080/19443994.2013.815687.

[4] S. Kaur, S. Rani, and R. K. Mahajan, "Adsorption Kinetics for the Removal of Hazardous Dye Congo Red by Biowaste Materials as Adsorbents," *J. Chem.*, 2013, doi: 10.1155/2013/628582.

[5] T. P. M. Chu *et al.*, "Synthesis, characterization, and modification of alumina nanoparticles for cationic dye removal," *Materials (Basel).*, 2019, doi: 10.3390/ma12030450.

[6] V. Karthik, K. Saravanan, P. Bharathi, V. Dharanya, and C. Meiaraj, "An overview of treatments for the removal of textile dyes," *Journal of Chemical and Pharmaceutical Sciences*. 2014.

[7] Á. de J. Ruíz-Baltazar, S. Y. Reyes-López, M. de L. Mondragón-Sánchez, A. I. Robles-Cortés, and R. Pérez, "Eco-friendly synthesis of Fe 3 O 4 nanoparticles: Evaluation of their catalytic activity in methylene blue degradation by kinetic adsorption models," *Results Phys.*, 2019, doi: 10.1016/j.rinp.2018.12.037.
[8] E. Aghaei, R. D. Alorro, A. N. Encila, and K. Yoo, "Magnetic adsorbents for the recovery of precious metals from leach solutions and wastewater," *Metals*. 2017, doi: 10.3390/met7120529.
[9] A. A. Farghali, M. Bahgat, A. Enaiet Allah, and M. H. Khedr, "Adsorption of Pb(II) ions from aqueous solutions using copper oxide nanostructures," *Beni-Suef Univ. J. Basic Appl. Sci.*, 2013, doi: 10.1016/j.bjbas.2013.01.001.
[10] M. Ghulam, T. Hajira, S. Muhammad, and A. Nasir, "Synthesis and characterization of cupric oxide (CuO) nanoparticles and their application for the removal of dyes," *African J. Biotechnol.*, 2013, doi: 10.5897/ajb2013.13058.
[11] M. S. Anitha S., Krishna B.M., Nagabhushana B.M., Sahana M., *No TitleNano CuO as Adsorbent for Color Removal from Textile Wastewater*. .
[12] M. F. Naouel Hezil, "Synthesis and structural and mechanical properties of nanobioceramic (α-Al2O3)," *J. Aust. Ceram. Soc.*, vol. 55, no. 4, pp. 1167–1175, 2019.
[13] L. B. Shi, P. F. Tang, W. Zhang, Y. P. Zhao, L. C. Zhang, and H. Zhang, "Green synthesis of CuO nanoparticles using Cassia auriculata leaf extract and in vitro evaluation of their biocompatibility with rheumatoid arthritis macrophages (RAW 264.7)," *Trop. J. Pharm. Res.*, 2017, doi: 10.4314/tjpr.v16i1.25.
[14] S. Nethaji, A. Sivasamy, and A. B. Mandal, "Adsorption isotherms, kinetics and mechanism for the adsorption of cationic and anionic dyes onto carbonaceous particles prepared from Juglans regia shell biomass," *Int. J. Environ. Sci. Technol.*, 2013, doi: 10.1007/s13762-012-0112-0.
[15] Y. C. Chang and D. H. Chen, "Recovery of gold(III) ions by a chitosancoated magnetic nano-adsorbent," *Gold Bull.*, 2006, doi: 10.1007/BF03215536.
[16] A. G. Mohamed Sulyman, Jacek Namiesnik, "Low-cost Adsorbents Derived from Agricultural By-products/Wastes for Enhancing Contaminant Uptakes from Wastewater: A Review," *Polish Kournal Environ. Stud.*, vol. 26, no. 2, pp. 479–510, 2017.
[17] A. A.-Z. Muhammad A.Rauf, I.Shehadeh, Amal Ahmed, "Removal of Methylene Blue from Aqueous Solution by Using Gypsum as a Low Cost Adsorbent," *Int. J. Chem. Mol. Eng.*, vol. 3, no. 7, 2009.